7
On-line Monitoring of Reaction Kinetics in Microreactors Using Mass Spectrometry and Micro-NMR Spectroscopy

Jacob Bart and Han Gardeniers

7.1
Introduction

Mass spectrometry (MS) and nuclear magnetic resonance (NMR) spectroscopy are well-established techniques for the identification of chemical compounds. Both methods deliver unique fingerprints of molecules and, under the right conditions, they can also be used to quantify the concentration of a compound in a mixture, if not too many substances are present with spectra that show overlapping signals. Mostly the methods are used for pure substances, although and over recent decades, the techniques have particularly been used to study biomolecules such as peptides and proteins. For mixtures of, say, more than five compounds, an analytical separation method such as electrophoresis or chromatography is required to be able to identify or quantify the compounds.

The basic principle of NMR consists in the measurement of the resonance of nuclear spins, present in a large and uniform magnetic field, where the resonance is excited and detected with radiofrequency (RF) transmitters. The resonance (for example of protons, ^{1}H, one of the most frequently studied atoms with a nuclear spin), depends on the electronic environment of the specific nucleus in a molecule and on the magnetic moments induced by the adjacency of other nuclear spins. The electronic effects are expressed in a so-called chemical shift, in parts per million (ppm), which is the parameter by which NMR spectra are usually plotted. The intensity of a specific resonance (i.e. the peak area in the spectrum) is proportional to the amount of spins with that resonance and can therefore be used as a (relative) measure of the concentration of the species to which the nuclear spins belong. The presence of other spins is generally found back in a splitting of the peaks (so-called *J*-coupling) or in cross peaks in two-dimensional NMR. The interpretation of NMR spectra and the special procedures to extract information from a nuclear spin system and also the (quantum mechanical) origin of NMR will not be discussed here; we refer the interested reader to one of the many textbooks that exist on these topics (see e.g. [1]).

Micro Process Engineering, Vol. 3: System, Process and Plant Engineering
Edited by V. Hessel, A. Renken, J.C. Schouten, and J.-I. Yoshida

ISBN: 978-3-527-31550-5

The principle of MS exists in ionizing molecules, passing the resulting ions through electric and/or magnetic fields of special configuration which separate the ions based on their mass-to-charge ratio (m/z) and focus them on an ion-sensitive detector which determines the amount of ions with the specific m/z value. Identification of a compound is thus performed by determining its mass. More sophisticated MS equipment has the possibility to fragment chosen compounds from a mixture, which can give a more accurate identification of the compound, provided that it can be compared with a standard of a known compound or to spectra collected in an MS databank. Quantification depends very much on the ionization process used, a topic that will be discussed briefly in this chapter. For more details about MS and the available equipment configurations, we refer to one of the many textbooks available (see e.g. [2]).

In this chapter, we will focus on NMR and MS on small-volume samples, of a few nanoliters to a few microliters, of which the composition needs to be analyzed in order to follow a chemical reaction in time. Such samples can therefore be either small fractions extracted from a larger (but still micro-) reactor or they can be the total volume of the microreactor itself. In the first case, the reaction in the fraction may have to be quenched in order to account for the time interval (and different conditions) during transport of the fraction from reactor to analyzer; in the second case, the microreactor needs to be integrated with the spectrometer in a reliable way. The manipulation and analysis of such small samples require special technical implementations and adjustments to the spectrometric equipment, which is the main topic of this chapter.

7.2 On-line Monitoring by Micro-NMR Spectroscopy

7.2.1 Introduction

Since its discovery in 1946, NMR spectroscopy has rapidly advanced as an interdisciplinary technique that employs the principles of chemistry, physics, engineering, medicine and biology. NMR spectroscopy has become one of the major analytical techniques for elucidation of chemical structure in both the liquid and solid phases.

As practitioners of the chemical sciences continue to blur disciplinary boundaries through investigations of more complex systems, analytical methods must correspondingly increase in their degree of sophistication. For example, still more groups are combining chemical separation techniques such as liquid chromatography (LC) and capillary electrophoresis (CE) with analytical sensing techniques such as NMR and MS. LC and CE are powerful methods to separate efficiently extremely small sample volumes. Along with the ability to inject and separate nanoliter volumes, the availability of a detection scheme capable of working with such small-volume samples is important. To be compatible with these techniques, there is a need for NMR on lower sample volumes in the order of microliters and even nanoliters. Furthermore, within the microreactor chemistry, there is a growing interest in onboard-placed chemical sensors because this opens the way to in-flow monitored production processes of high-grade compounds executed on one chip. The research

and development of NMR microprobes and the sensitivity advances of microprobes have had a tremendous impact on the capabilities of NMR as a detection mechanism for chemical techniques using mass-limited samples.

7.2.2 NMR Sensitivity

The main limitation in NMR is the fact that the low energy scales inevitably lead to rather low sensitivity. Only with the utmost care in noise reduction can the spectra or images be accumulated in a reasonable amount of time. Even then, the technique demands rather high spin concentrations.

The signal-to-noise ratio (SNR) of an NMR experiment was initially formulated by Abragam [3] and the analysis was extended by Hoult and Richards [4]. It can be written mathematically as

$$\mathrm{SNR} = \frac{k_0\left(\frac{B_1}{i}\right) V_\mathrm{s} N \gamma \hbar^2 I(I+1) \frac{\omega_0^2}{k_\mathrm{B} T \times 3\sqrt{2}}}{F\sqrt{4 k_\mathrm{B} T R_\mathrm{noise} \Delta f}} \tag{7.1}$$

where k_0 is a scaling factor accounting for the RF inhomogeneity of the coil, B_1/i the magnetic field induced in the RF coil per unit current, V_s the sample volume, N the number of spins per unit volume, γ the gyromagnetic ratio, I the spin quantum number, ω_0 the nuclear Larmor precession frequency, T the absolute temperature and h and k_B Planck's and Boltzmann's constant, respectively. The denominator describes the noise using the noise factor of the spectrometer F, conductive losses of the coil, circuit and sample R_noise and the spectral bandwidth Δf. Collecting all the natural constants in the constant C, the SNR is thus given by the simple expression

$$\mathrm{SNR} = C \frac{\left(\frac{B_1}{i}\right) V_\mathrm{s} N}{\sqrt{R_\mathrm{noise} \Delta f}} \tag{7.2}$$

By analyzing these equations further, Richards and Hoult stated that the sensitivity of RF coils increases when the size and shape of the RF coil match the sample [thus maximizing $(B_1/i)V_\mathrm{s}N$], which provides a high coefficient of magnetic field coupling between the coil and the sample. The optimum experimental set-up is to dissolve the sample in the minimum volume of solvent and to construct the smallest RF coil that will enclose the sample. Thus, the SNR of an NMR experiment can be increased by concentrating the sample (keeping the same amount of sample in a smaller volume) and matching the coil shape to this decreased volume. This means that for mass-limited samples the total data acquisition time can be reduced significantly by means of microcoil NMR probes, for achieving the same SNR [5].

7.2.3 Spectral Resolution

7.2.3.1 Probe-induced Line Broadening

The main factor that limits the performance of micro-NMR-probes in terms of sensitivity and spectral resolution is identified as probe-induced static magnetic field

inhomogeneity. One of the disadvantages of placing the coil in close proximity to the sample is that significant susceptibility-induced line broadening occurs. Line broadening shows up when the B_0 homogeneity is disrupted by materials of different susceptibility near the sample. This phenomenon will not only decrease the resolution of the experiment (broader spectral lines) but also decrease the sensitivity, as the integral under one peak will be the same for the same number of spins. Olson *et al.* [6] showed that both sensitivity and resolution can be improved significantly by immersing the used copper excitation coil in perfluorocarbon FC-43 (Fluorinert), having nearly the same susceptibility as copper. In that case, the sample is surrounded by a homogeneous susceptibility cylinder; according to electromagnetic field theory, a sample enclosed by a perfectly uniform and infinitely long hollow cylinder experiences a uniform static magnetic field [7].

7.2.3.2 **Sample-induced Line Broadening**

A second source of magnetic field distortions is the discontinuity in susceptibility at both ends of the sample, which in a conventional NMR tube is typically shaped as a cylindrical plug. To minimize field distortions in the observed volume of the coil, the plug length should be significantly longer than the coil length, the *infinitely long sample* approach [5]. This arrangement places most of the sample outside the observed volume, thus lowering the sample sensitivity.

An approach to avoid either sample waste or sample-induced line broadening is to use susceptibility-matched plugs which are placed at both ends of the sample plug. This technique is broadly used for conventional probes [8], but Behnia and Webb [9] showed that this technique will also work for nanoliter samples in capillaries. They demonstrated spectra of 5% H_2O–95% D_2O in different sample configurations in a 1.4 mm long solenoid. For a 2 mm long air-bracketed sample in a capillary, they achieved linewidths of 6.4 Hz (0.026 ppm). By bracketing the 2 mm long sample plug on both sides by FC-43 (Fluorinert) liquid they obtained an improved linewidth of 1.4 Hz (0.0056 ppm).

Although these results give insight into the sources of susceptibility broadening, they will not be very relevant for in-flow experiments, because in that situation the *infinitely long sample* constraint can be easily fulfilled.

7.2.4
Approaches to High-resolution Micro-NMR

7.2.4.1 **Solenoids**

The first attempt at high-resolution NMR performed on sample volumes down to 5 nL was published by Wu *et al.* [10, 11]. A solenoidal microcoil wrapped directly around a fused-silica capillary containing 5 nL of sample is placed in a conventional superconducting magnet. The coil is used as a detection system for LC. With a thin-walled capillary (145 μm i.d.) they obtained linewidths over 200 Hz (0.73 ppm) for a 0.8 M sample of arginine, whereas for a thick-walled capillary (350 μm o.d.) the linewidths were narrowed to 11 Hz (0.037 ppm). This is according to the probe-induced susceptibility broadening described above. Although the minimally detectable numbers of spins

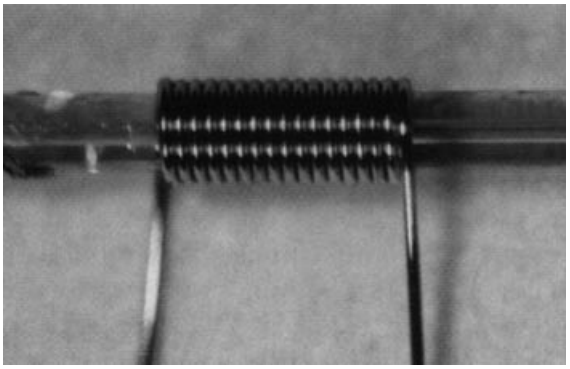

Figure 7.1 Microcoil wrapped around fused-silica capillary. The coil is composed of 50 µm-diameter copper wire and has a length of 1 mm and an o.d. of 470 µm. Reproduced with permission from [6].

from these microcoils were considerably better than those achieved with standard probes, the linewidths of the order of 10–20 Hz are unacceptable for high-resolution NMR spectroscopy. The first high-resolution NMR spectra were presented by Olson *et al.* [6], who employed the same design (Figure 7.1) but, by using the magnetic susceptibility compensation mentioned above, were able to obtain linewidths of 0.6 Hz (0.002 ppm) full width at half-maximum (FWHM) on a sample of pure ethylbenzene. This concept has been optimized and probes working as such are now commercially available under the name CapNMR [12–14]. The probes are currently used for in-flow NMR [15] and in-flow LC–NMR [16] and as high-throughput NMR spectroscopic instruments, by coupling it to an HPLC pump and an autosampler [17].

7.2.4.2 **Planar Microcoils**

Not surprisingly, the fabrication of solenoidal RF microcoils is a manufacturing challenge, especially at smaller wire dimensions. An alternative to manually wrapping the wires around capillary tubes is to take advantage of lithographic fabrication techniques. Several groups have investigated planar microcoils as the modern way to perform NMR on nanoliter samples [18–24]. The first planar microcoil for NMR detection was demonstrated by Peck *et al.* [18], who patterned a GaAs substrate with gold inductors, using photolithographic and lift-off methods. An electron micrograph of the coil is shown in Figure 7.2. A silicone rubber (RTV) sample was placed directly over the coils. An SNR of ~20 (64 times averaged) and an FWHM of 60 Hz (0.2 ppm) were obtained.

A thorough study of the electrical and spectroscopic characteristics of planar microcoils was done by Massin an coworkers [23, 24], who characterized and optimized a microfluidic probe with a planar microcoil on a glass substrate. A 75 µm deep channel was etched in a Pyrex glass substrate and the NMR detection coil was integrated on the top surface of the microfluidic wafer stack, using a process based on SU-8 photoepoxy and copper electroplating. With this chip (depicted in Figure 7.3), containing a sample of 160 µg of sucrose in 470 nL of D_2O, they obtained a spectral SNR of 38 (16 times averaged) and an FWHM of 9 Hz (0.03 ppm) (see Figure 7.4).

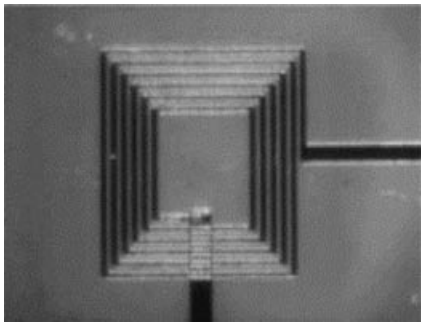

Figure 7.2 Electron micrograph of the first planar microcoil. The o.d. is 200 µm. Reproduced with permission from [25].

The fundamental disadvantage of these planar coils is the very inhomogeneous RF field, especially close to the coil, where the RF field is strong. To avoid this drawback, several groups have investigated Helmholtz coils [26–27]. Ehrmann *et al.* [28] recently published a (2×4 turns, 240 µm i.d.) Helmholtz-based micro-NMR probe, with integrated microfluidic channels in SU-8 on a Pyrex substrate. This concept is drawn schematically in Figure 7.5. The coils were fabricated by electroplating. For a 9-nL pure water sample they obtained a spectral SNR of 620 and a linewidth of 5 Hz (0.017 ppm).

7.2.5 On-line NMR Monitoring

During the last two decades, hyphenated analytical techniques have become fairly commonplace. Multimode separation and detection strategies are required in such

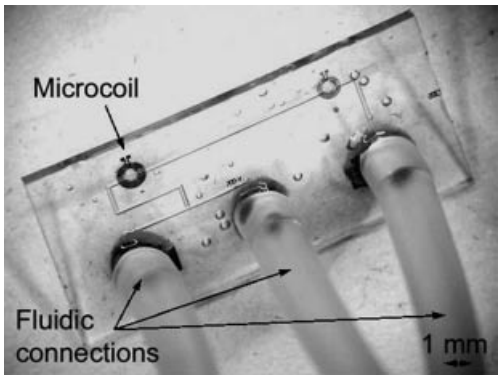

Figure 7.3 Picture of a micromachined planar NMR probe. The glass chip has a size of $16 \times 8\,mm^2$. The visible microfluidic channels have a width of approximately 170 µm. The pointed microcoil has an i.d. of 500 µm and an observed volume of 30 nL. The sample is injected via flexible plastic tubes connected to inlet and outlet holes on the back side of the chip. Note that several coils may easily be integrated on a single chip. Reproduced with permission from [22].

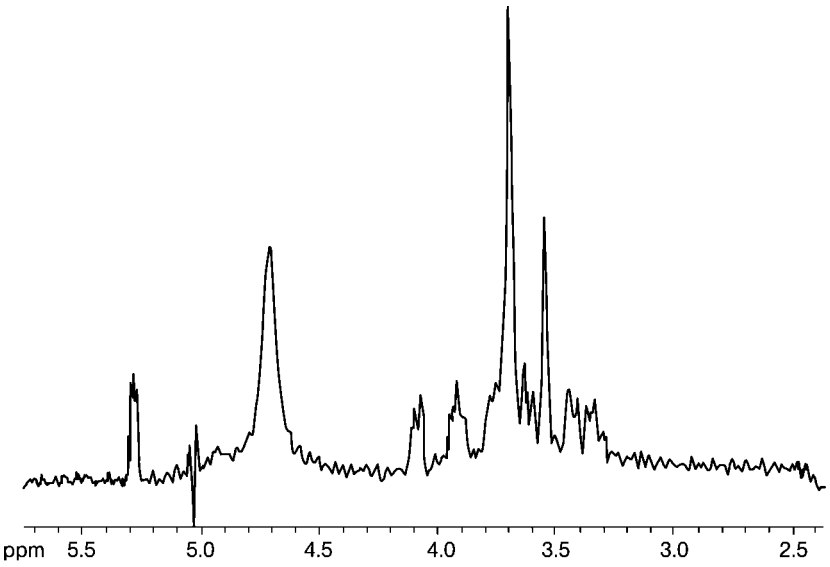

Figure 7.4 ^{1}H NMR spectrum of 160 µg of sucrose in 470 nL of D_2O after Lorentz–Gauss resolution enhancement. The resulting spectrum has a Gaussian lineshape with FWHM ≈9 Hz and $SNR_f \approx 38$ (anomeric proton), for 16 acquisitions. Reproduced with permission from [24].

diverse areas as characterization of pharmaceutical candidates, understanding chemical communication within living organisms and geochemical analysis of planetary samples. In particular, NMR has been coupled to separation methods such as LC and CE and used as a method to follow reaction kinetics.

Having developed microcoils on a substrate, it is only one step further to integrate more than one microfluidic channel in the substrate on which the planar coil is placed, for example in order to study reaction kinetics. Developments in silicon and glass microfabrication technology have increased rapidly and integration of different chemical unit processes can be made easier by the use of modern microfabrication.

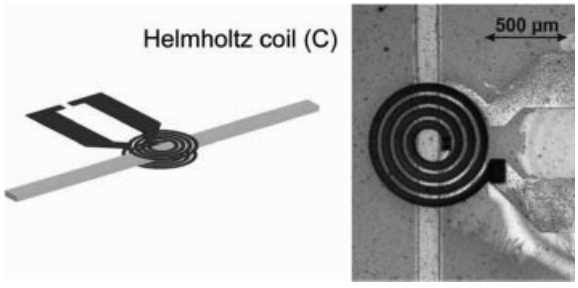

Figure 7.5 Design derived from mask layout and picture of fabricated Helmholtz coil. Reproduced with permission from [28].

7.2.5.1 Flow Effects

In 1984, Laude and Wilkins reported a systematic study of the effects of flow rates on both NMR sensitivity and resolution for analytical-scale HPLC–NMR [29]. Flow of analyte through the detection coil reduces the effective longitudinal relaxation time of the sample by replacing pulsed spins with unpulsed spins, thereby allowing more rapid pulse repetition and improved SNR per unit time. This means that provided that the analyte in the probe does not change, sample flow through the probe has a positive effect on the SNR. However, when NMR is used as a detection method for in-flow separation detection, pulse repetition for averaging is not always possible, because of the sample composition change (the peaks in a chromatogram, for example), which should be followed by the coil. In that case, the flow rate will put constraints on the SNR, which depends very much on the analyte peak width at the location of the coil. Since miniaturized separation systems generally are faster and therefore exhibit less peak broadening by diffusion dispersion than conventional separation systems, this may constitute a problem for further down-scaling of such systems in combination with NMR.

Regarding resolution under flow conditions, it has to be taken into account that the spin residence time will be limited. This may increase the signal linewidth for any given analyte spin not observed for a period long enough to allow full signal decay within the observe volume of the NMR probe. In this case, the effective transverse relaxation time of the analyte decreases in a flowing system and the signal decays more rapidly (and in a different way) than for a static analysis. The resulting increase in linewidth due to flow is inversely proportional to the residence time [30, 31]. Consequently, although higher flow rates allow faster pulse repetition and a possible increase in SNR, the degradation in linewidth may conceal important spectral information. As a result, the optimum flow rate for on-line NMR detection is a compromise between SNR, linewidth and kinetics/chromatographic resolution.

7.2.5.2 NMR Detection of Capillary Separations: LC–NMR

Conventional LC–NMR employs separation columns which are connected to NMR detection probes via open tubular capillaries with internal diameters substantially smaller than the column to avoid extra-column band broadening. Since the band broadening introduced by the connections and transfer lines causes significant peak dispersion in capillary separations, on-column detection for small-volume LC is desirable. Because of the need for deuterated solvents for NMR detection, the relatively large volumes and flow rates used with conventional analytical HPLC columns make coupling of LC and NMR an expensive experiment.

The principal drawback with these approaches has been the relatively poor mass sensitivity of the NMR detection system, especially when the observation time is limited for each analyte peak. To minimize this, one can employ more concentrated samples, combined with smaller diameter chromatographic columns to minimize solvent consumption and maximize NMR sensitivity.

The first microbore LC–NMR experimental results were published in 1995 [32]. In this report, a solenoidal microcoil was wrapped around a fused-silica capillary (50 nL), directly connected to an LC microbore column, situated in the bore of the

magnet. They were able to detect the separation of three amino acids and two peptides with concentrations in the submicrogram range. Currently, micro-HPLC–NMR probes are commercially available [13].

7.2.5.3 NMR Detection of Capillary Separations: CE–NMR

Capillary electrophoresis (CE) is a powerful method capable of efficient separations of extremely small-volume samples. Because of the small sample volumes involved (nanoliters) in conventional CE, NMR as detection scheme for CE is not obvious, due to the inherent insensitivity of NMR. Developments in micro-NMR as described earlier have opened up new ways for NMR as a detection scheme for CE.

CE–NMR on nanoliter samples was first reported by Wu *et al.* [32] (see also the section on solenoids). They observed a separation efficiency of ~5000 theoretical plates for cysteine, poor for CE but comparable to the best reported LC–NMR results. Further publications on this subject have shown the capabilities of the combination of CE and micro-NMR [33–35].

The combination of chip-based CE with NMR was first demonstrated by Trumbull *et al.* [19], who integrated a planar NMR coil on a CE chip. They accomplished CE separations in microfluidic devices, but satisfactory NMR spectra could only be obtained from samples of high concentration.

Despite relatively simple instrumental requirements, CE–NMR data reflect a complex interdependence on flow rate, electric field and current [35]. For instance, the current which passes through the capillary produces a magnetic field gradient that may perturb the uniformity of the B_0 field if it cannot be counteracted through shimming. This flow-dependent line broadening can be solved by use of periodic stopped flow.

7.2.5.4 Reaction Kinetics

Knowledge of kinetics is an important component in investigating reaction mechanisms. NMR has been used for the direct observation of short-lived species in chemical reactions by using rapid injection [36] and continuous-flow techniques [37]. Ciobanu *et al.* [38] studied continuous reactant flow combined with multiple microcoil NMR detection to obtain kinetic information on reactions that take place on time scales between seconds and minutes. As a model system, they studied D-xylose–borate reaction kinetics. The ^{1}H NMR spectra of D-xylose (300 mM) and the equilibrium mixture of D-xylose plus borate (400 mM, pD 10) solutions are shown in Figure 7.6a and b, respectively (no flow). The reactants are mixed and this mixture is passed through a capillary with three physically distinct NMR solenoidal microcoils wrapped around it. The distance between the mixer and each individual NMR coil, together with the flow rate used, determines the post-reaction time point. As the reaction progresses, a decrease in the height of the α and β anomeric peaks and the appearance of a new peak (denoted product anomeric in Figure 7.6b), at 5.55 ppm are observed. NMR spectra that correspond to successive reaction times were recorded independently and simultaneously with all three RF coils. Figure 7.7 depicts the results from a quantitative analysis of the spectra. This work demonstrated the possibility of using NMR as an analytical tool to study the chemical kinetics of small

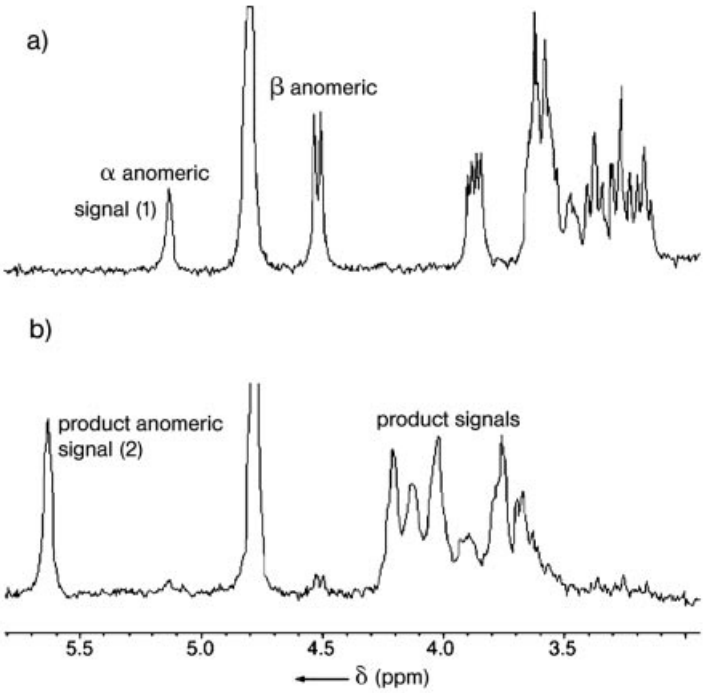

Figure 7.6 ^{1}H NMR spectra of 300 mM (a) D-xylose in D_2O and (b) D-xylose plus 400 mM borate at pD 10. The spectrum in (b) corresponds to the equilibrated product mixture. Chemical shifts are referenced to HDO at 4.78 ppm. Reproduced with permission from [38].

amounts of materials with reaction times of a few seconds or longer by continuous-flow NMR. Continuous flow decouples the total data measurement time from the reaction time, as averaging is possible because at constant flow the composition of the sample in the detection coil is always the same. Furthermore, the use of multiple microcoils decreases the amount of sample required to obtain the data.

Wensink *et al.* presented a microfluidic chip with an integrated planar microcoil for samples with volumes of 56 nL [39] (Figure 7.8). Real-time monitoring of imine formation from benzaldehyde and aniline in the microreactor chip by NMR was demonstrated at 1.4 T (60 MHz). Two liquids are injected into the two inlets of the chip by use of programmable syringe pumps. The flow rate determines the residence time in the channel section between the mixing point and the detection area and this residence time is taken as the reaction time. By changing the liquid flow speed, the reaction times in the chip can be set from 30 min down to ca. 2 s (which is close to the time required for mixing of the two reactants). Figure 7.9 shows the increase in the imine peak and decrease in the aldehyde signal with increasing residence time. The peak areas of the two peaks of interest were calculated to follow the course of the reaction. In Figure 7.10, the conversion of the reaction is plotted as the ratio of each

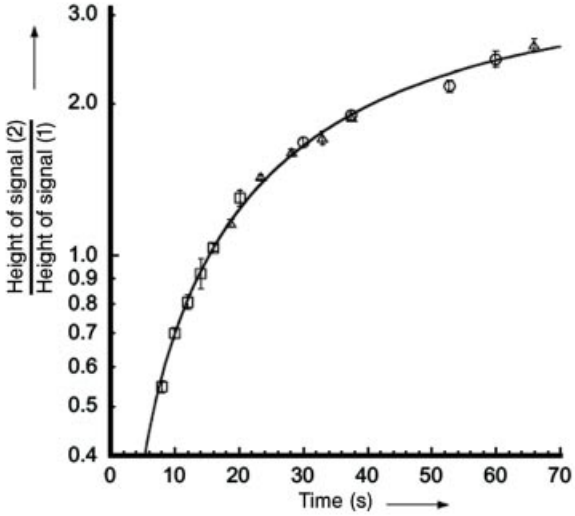

Figure 7.7 The ratio of the signal amplitudes, height of signal (2)/height of signal (1) (see Figure 7.6), as a function of time, for three solenoidal coils on a capillary. The coils are ~20 cm apart, in the order coil 1 (□) – coil 2 (△) – coil 3 (○). Reproduced with permission from [38].

peak area to the sum of both peak areas, as a function of the residence time. The results could be fitted with a second-order rate equation with a rate constant of $6.6 \times 10^{-2}\,M^{-1}\,min^{-1}$, with a correlation coefficient of 0.93. Interestingly, the same reaction carried out in a conventional probe in a 400-MHz NMR machine using the same concentration as in the chip gave a second-order rate constant of $(3.35 \pm 0.05) \times 10^{-2}\,M^{-1}\,min^{-1}$. In that experiment, the reaction was followed by taking a single scan every 5 s and the

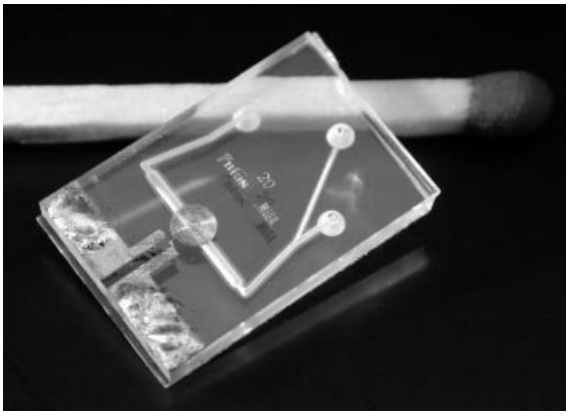

Figure 7.8 NMR glass chip with planar copper microcoil. Chip size, 1 × 1.5 cm; channel width underneath coil, 500 μm [39].

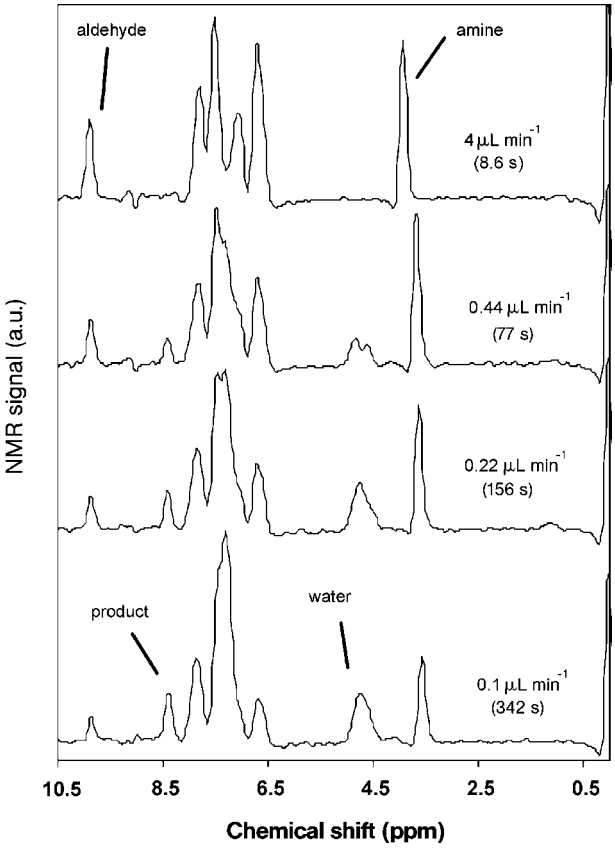

Figure 7.9 ^{1}H NMR spectra taken at different residence times for the reaction of benzaldehyde with aniline [39].

experiment was performed three times. The two times higher reaction rate constant found in the chip is attributed to a better mixing performance in the chip.

Recently, a 5-mm compatible microchanneled cell for synthesis monitoring (MICCS) was brought on the market by Jeol [40, 41]. This long chip, which fits in a standard 5-mm sample tube, contains 300 µm wide and 100 µm deep reaction channels with an 8-µL observed volume. Measurements have to be performed with the standard saddle-coil in a 5-mm probe. Takahashi *et al.* [41] were able to show the intermediates which appear during the reaction of the Grignard reaction of 3-hexen-2-one with CH_3MgBr in tetrahydrofuran (THF). Both solutions are mixed in the Y-shaped channel and the flow rates are changed to probe the different reaction stages involved. ^{1}H NMR spectra are recorded every minute.

7.2.5.5 **Protein Folding Kinetics**

NMR has already been used for several years to study protein folding [42, 43]. Kakuta *et al.* [44] improved the performance of NMR studies directly applied to protein folding kinetics using advances in microfluidics and microcoils. They studied changes in

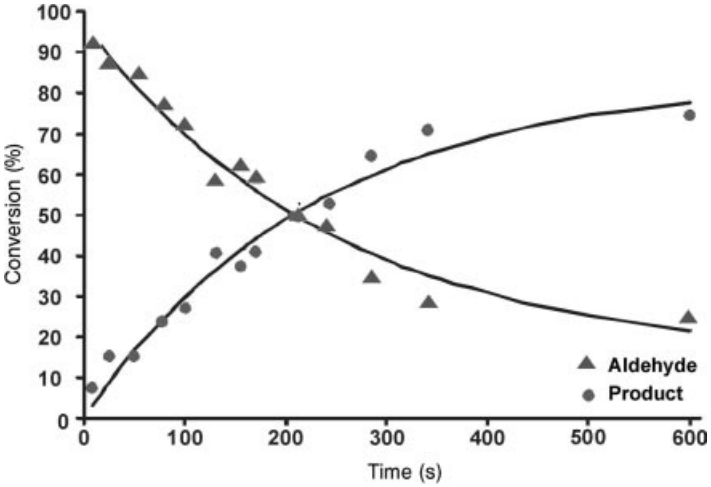

Figure 7.10 Conversion in terms of percentage product formation and percentage of benzaldehyde converted, calculated from a series of NMR spectra as shown in Figure 7.9 [39].

protein conformation based on the elapsed time after a change in the solvent composition by use of a micromixer (either a Y-connector or a micromachined micromixer [45]) coupled directly to a solenoidal microcoil wrapped around a fused-silica capillary (250 µm i.d./350 µm o.d.) containing 800 nL of sample. They demonstrated time-resolved NMR spectroscopy for studying the real-time methanol-induced conformation changes of ubiquitin. Under acidic conditions, methanol induces a transition from a native to a partially unfolded state, the A-state. His68 and Tyr59 were used as proton NMR probes to follow such conformational changes. The ubiquitin transitions at different time intervals were controlled by mixing a 20% CD_3OD–80% D_2O and 7 mM ubiquitin (pD = 2.4) solution with 80% CD_3OD–20% D_2O (pD = 2.4) at different flow rates from 2 to 60 µL min^{-1}, corresponding to times of 114–3.8 s.

Figure 7.11 shows selected NMR spectra recorded at different flow rates using the Y-connector. Peaks a and b are assigned to ubiquitin His68 (C_4 proton) in the native and the A-state, respectively. Similarly, peaks c and d are assigned to native and A-state of Tyr59 (meta protons), respectively. The time-dependent behavior of these two states was quantified as the population ratio of the A-state to the native state and is shown in Figure 7.12.

7.3
Monitoring of Reaction Kinetics Using MS

7.3.1
Introduction

In contrast to NMR, which is a non-destructive analytical technique, MS requires ionization and in many cases also fragmentation of molecules in order to perform an

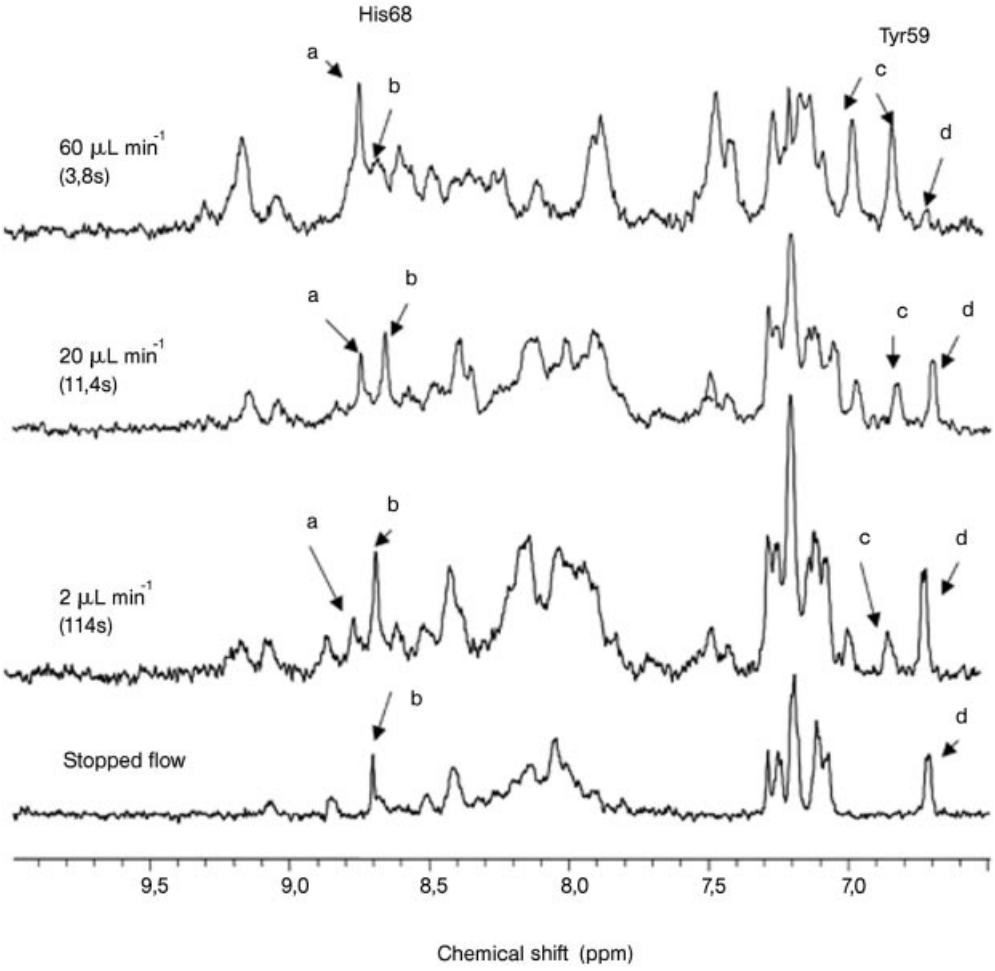

Figure 7.11 Spectra from the Y-connector with stopped flow and at various flow rates (mixing times): stopped flow, 2 (114 s), 20 (11.4 s) and 60 µL min^{-1} (3.8 s). The labeled peaks correspond to (a) native state His68, (b) A-state His68 and (c) native state Tyr59. Reproduced with permission from [44].

analysis of their mass or structure. This is why in some continuous flow capillary-based set-ups a mass spectrometer is coupled *after* LC–NMR [46], although in most cases NMR and MS are used in parallel after LC (see e.g. [47] as one of the first examples), a set-up that is available nowadays as a complete solution from several suppliers (e.g. Bruker and Varian).

If one compares MS and NMR for studying chemical reactions and their products, a few typical differences become clear. For structural information, in particular on a three-dimensional molecular configuration, NMR is certainly the preferred method, through the possibilities offered by techniques such as NOESY and more advanced

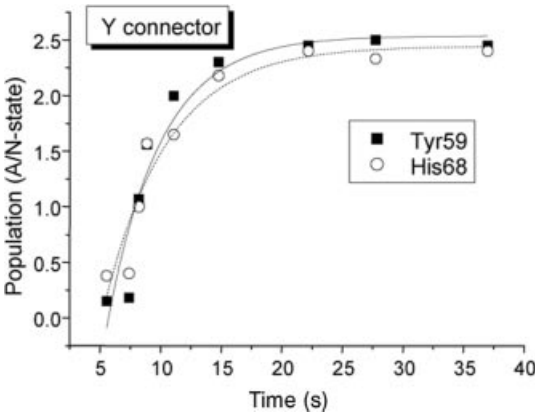

Figure 7.12 Kinetic data using the Y-connector. Reproduced with permission from [44].

pulsed NMR procedures [48, 49]. NMR is also a technique that can be performed directly on the sample, whereas all MS techniques require extraction of a (fraction of) sample before analysis, which makes MS more an in-line than an on-line technique. However, MS is far more sensitive than NMR, with a limit of detection in the attomole range, compared with tens of nanomoles to micromoles for NMR. Only with the recent developments in microcoil NMR, as discussed in the previous section, could a sensitivity in the picomolar range be obtained for ^{1}H NMR [9]. Another important advantage of MS over NMR is that NMR works for only a limited number of elements, namely those that exhibit nuclear spin, whereas MS is unlimited in that respect. Finally, there still is a considerable price difference between NMR and MS equipment, of a factor of about 2–5 in favor of MS, where MS equipment can in fact be even less inexpensive if the required mass analysis range is not too large. The latter is the case for GC–MS applications in gas-phase reactions, which is the topic of the next section.

7.3.2
Gas-phase Reactions in Microreactors Studied by MS

MS is frequently used to monitor the progress of gas-phase reactions, in particular heterogeneous catalytic processes. In some cases the outlet gas is first fed through a gas chromatograph to separate components and determine their relative concentrations, before analyzing their mass for identification of the species present.

In the field of microreactors, two main configurations exist, one being the direct coupling of the outlet of a single microreactor to a GC–MS system, such as via a capillary, which is made compatible with the flow requirements of the GC–MS system. An example of this concept can be found in the work of Besser and coworkers, who applied on-line GC–MS for kinetic studies of the preferential oxidation of CO in silicon microreactors the microchannel walls of which were covered with a thin-film catalyst [50]. The outlets of four silicon microreactors running in parallel are fed

either into a gas chromatograph for quantification or MS for identification, via several valves and tubing.

Another interesting example is the microfabrication of a 10 μm diameter capillary leak in a silicon micro-flow system, to provide a gas route to a mass spectrometer [51]. The use of an integrated capillary leak minimizes dead volumes in the system, resulting in increased sensitivity and reduced response time for the intended use of the microdevice for temperature-programmed desorption (TPD) of CO desorbing from platinum. It is shown that CO desorbing in 105 Pa of argon as a carrier gas from as little as 0.5 cm^2 of platinum foil gives a clear desorption peak, a sensitivity approaching that of TPD experiments in vacuum.

A second configuration that is used for high-throughput screening of heterogeneous catalyst libraries consists in the use of a sniffler nozzle to scan the outlets of microchannel reactors. The basic configuration is shown in Figure 7.13. This configuration was used by Senkan and Ozturk for time-on-stream testing of a combinatorial Pt/Pd/In catalyst library with 66 combinations for the catalytic dehydrogenation of cyclohexane to benzene, in a microreactor array [53]. Claus *et al.* used the set-up with two different reactor configurations with different degrees of miniaturization (viz. a monolithic multichannel reactor and a silicon micromachined microreaction system) for the parallel and fast screening of heterogeneously catalyzed gas-phase reactions, such as the oxidation of methane, the oxidation of CO and the oxidative dehydrogenation of isobutane [52]. For both microreactor configurations, quantitative product analysis could be achieved within 60 s per catalyst. Scanning MS was also applied to a multibatch reactor consisting of a number of parallel mini-autoclaves in which the liquid-phase hydrogenation of citral was investigated [52].

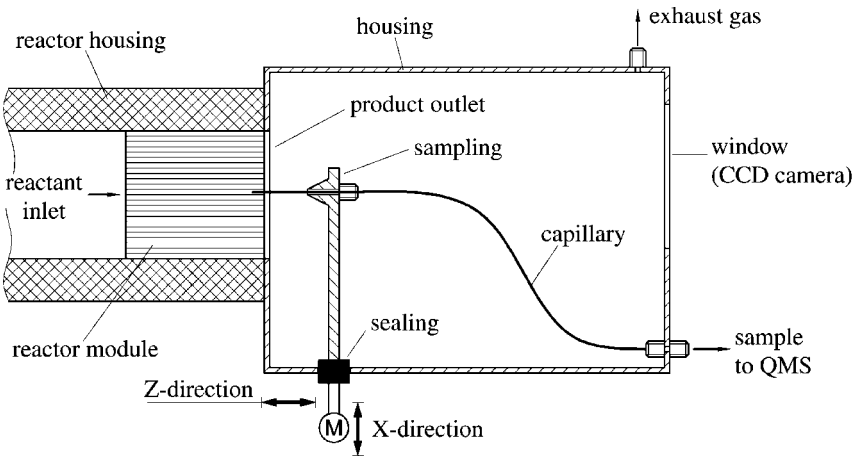

Figure 7.13 Schematic drawing of a multi-channel microreactor set-up of which the products are scanned with a nozzle, connected to a quadrupole mass spectrometer. Reprinted from [52], Copyright 2001, with permission from Elsevier.

7.3.3
Liquid-phase Reactions Using an Electrospray Interface to MS

Nowadays, interfacing separation methods such as high-performance liquid chromatography (HPLC) or CE [54] to MS is already a routine technique. MS methods based on so-called *soft ionization* techniques, which include fast atom bombardment, laser desorption and electrospray ionization (ESI), have allowed the analysis of biological macromolecules that in the past could have been analyzed only by extensive cleavage and derivatization. Of these methods, the two most preferred for biomolecules are ESI [55] and matrix-assisted laser desorption/ionization (MALDI) [56, 57], for which time-of-flight (TOF) and ion trap mass analyzers are the most frequently used mass analysis methods. However, these methods are equally suitable for small molecules, such as metabolites or the products of organochemical reactions.

The level of integration of MS coupling with the microreactor in the previous section on gas analysis by MS is not very high. This is different for most cases in which ESI is used. An ESI nozzle (see Figure 7.14 for a number of different configurations) gives the most convenient interface for on-line monitoring of liquid-phase chemistry. It is the preferred method for coupling LC and CE applications to MS. It has also been used frequently to study the kinetics of enzymatic reactions in capillary systems (see [58] for a recent review) and nowadays also in chip-based microreactor systems.

Microreactors in chip format provide an excellent means to perform sample preparation for mass spectrometers [59]. The mass spectrometer and the microchip are well matched, due to the similarity in flow rates generated by a microchip with those required for ESI-MS, for example. Examples of early work on chip-coupled ESI are electrospray directly from the edge of a planar glass chip (see Figure 7.14a), where the liquid to be analyzed exits the separation channel, either driven by electroosmotic flow (EOF) [60] or by hydraulic pressure [61]. For coupling to CE on a chip, better results were obtained with a sharpened and metal-coated capillary, attached to the end of the chip, as an ESI interface [62]. Recent developments are ESI nozzles integrated with a chip, such as a microfabricated nozzle in-plane with the surface of a chip [63], and a chip with multiple nozzles, etched in silicon so as to generate electrospray perpendicular to the surface of a chip [64], and an LC chip with integrated ESI nozzle fabricated in plastic foils with the aid of laser ablation, which is implemented in a six-way HPLC valve and is commercially available from Agilent [65]. Interesting developments are microfluidic systems with parallel electrospray nozzles for multiplexed analysis, such as the eight-channel glass chip developed by the same group [66] (this device has no nozzles, but simply uses the open ends of microchannels) or the plastic microdevice with 96 electrospray nozzles (compatible with a 96-well titer plate) developed by Liu *et al.* [67]. More details about such multiplexed MS devices can be found in a review by Foret and Kusý [68].

The devices mentioned above were all developed for coupling of MS to separation columns. For application in LC and CE and particularly for miniaturized systems of this kind, a major source of peak dispersion originates from the connecting capillaries and fittings. This becomes critical when the ratio of peak volume to

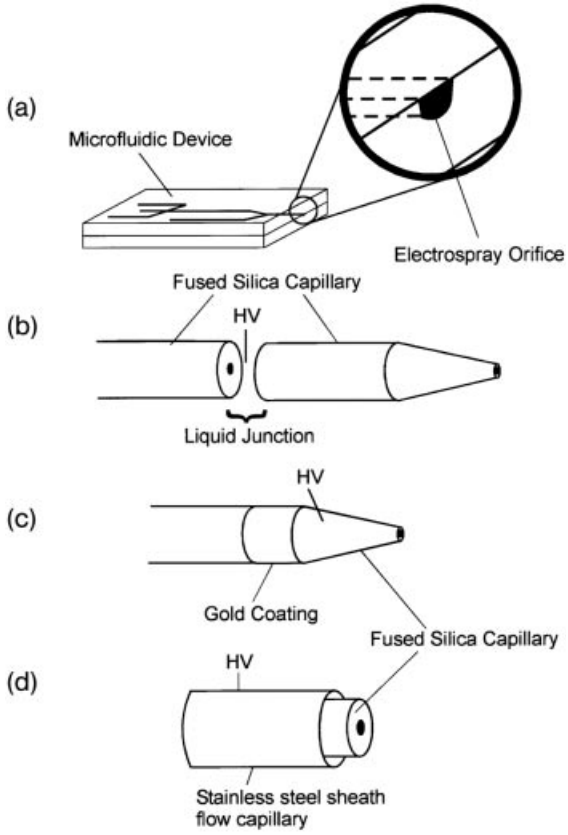

Figure 7.14 Different electrospray interfaces developed for chip-ESI-MS. (a) Spray directly from an open channel outlet at the edge of the chip; (b) liquid junction capillary interface; (c) gold-coated capillary interface; (d)) coaxial sheath flow configuration. HV denotes the points to which the electrospray voltage is applied. Reprinted from [59], Copyright 2000, with permission from Elsevier.

connecting dead volumes becomes too small. For those situations, integrated ESI nozzles are essential. However, for chemical reaction systems generally dead volumes in the connection to MS are less relevant. These dead volumes may change the residence time distribution for the reacting mixture somewhat, possibly in an unpredictable way, but generally the effect will be negligible, since the volume of the reacting mixture in most situations is at least the volume of the reactor, if not several times that volume.

An example of a microreactor coupled to ESI-MS is the glass chip developed by Brivio *et al.*, who studied the kinetics of different types of reactions, for example, metal–ligand interactions of zinc porphyrin with different pyridines and imidazoles and host–guest complexations of β-cyclodextrin with several compounds [69], and the

derivatization reaction of different isocyanates with 4-nitropiperazino-2,1,3-benzoxadiazole (NBDPZ) to yield the corresponding urea derivatives [70]. In the latter study, it was found that rate constants on the chip are 3–4 times higher than those determined using a laboratory-scale batch reactor, which was attributed to more efficient mixing in the microreactor chip. The microreactor chip was enclosed in a home-made chip holder which was configured with commercially available nanospray capillary tips, which provided the interface with the MS. In earlier work by Brivio *et al.* in which a glass microreactor chip was coupled to a nozzle, the outflow of which was collected on MALDI plates and analyzed by MS, it was found that in particular reactions the glass surface may act as a catalyst [71].

A similar configuration to that described above, using a chip holder with conventional electrospray tips, was used by Spikmans *et al.* for the on-line post-column derivatization of analytes, with the purpose of pre-ionization of these analytes [72]. In this set-up, the analytes are separated using gradient HPLC, subsequently derivatized in a micromixer chip and finally detected by ESI-MS. This approach solves one of the major limitations of ESI-MS, namely the dependence of detection on the degree of ionization. As a proof-of-principle, separated primary and secondary amines, and also ketones and aldehydes, are derivatized with a positively charged phosphonium complex. The fact that molecular cations are detected demonstrates that the ionization process is dominated by the phosphonium label, leading to more constant ionization for a variety of compounds. In addition, the use of a stable isotopically labeled ($^{12}C/^{13}C$) phosphonium reagent allows inherent improvement of the SNR and automated data processing using cluster analysis.

7.3.4
Liquid-phase Reactions Studied by MALDI-MS

MALDI is principally an off-line technique. The most common method consists in spotting the analytes, dissolved in a matrix solution, on a plate, where the matrix co-crystallizes with the analyte contained in its lattice. The function of the matrix is to adsorb the laser energy and transfer the resulting charge to the analyte, so that the analyte evaporates and can be transported by the electric field that is set up between the plate and the inlet of the mass spectrometer. Ionization usually takes place in a vacuum chamber, although atmospheric pressure (AP) MALDI exists; however, this method is not (yet) very well developed and less preferred because of the limited sensitivity and mass range.

The use of MALDI for quantitation of samples has frequently been questioned, because of the problem of obtaining a homogeneous matrix. However, this problem can be solved by the introduction of a standard compound which resembles the analyte chemically and calibration and averaging procedures. Despite these difficulties, MALDI has frequently been used for the quantification of substrates and products involved in enzyme-catalyzed reactions, in some cases even without the addition of an internal standard. This approach is based on the assumptions that signal intensity and concentration in MALDI samples is linear over a wide range of concentrations and that the responses for substrate and product are similar, so that

the sum of signal intensities at each point in time is equal to the signal intensity for the starting concentration of the substrate. Although these assumptions are not always justified, reasonably accurate results have been obtained (see e.g. [58] for a recent review).

Because of the off-line character of MALDI-MS, for the study of reaction kinetics the reaction in a sample to be analyzed has to be quenched at the desired time point, to allow for the transfer to the vacuum system of the MALDI equipment. In case of very fast reactions, this requires fast mixing of the reaction mixture with some quenching agent (e.g. an acid to denature and thereby inhibit an enzyme or neutralize a base catalyst; see below) and here micromixers may help. An example of this is recent work by Nichols and Gardeniers [73, 74], who used electro-wetting principles to "stir" and manipulate single droplets of reactants to study the pre-steady-state kinetics of a particular enzymatic reaction. Nichols and Gardeniers followed earlier work by Moon *et al.* [75] and Wheeler *et al.* [76, 77], who developed what they called an "integrated digital microfluidic chip", for multiplexed protein sample preparation and analysis by MALDI-MS. This chip uses a specific voltage sequence to generate a series of droplets from each of three reservoirs (proteomic sample, rinsing fluid and MALDI reagents), using electro-wetting principles in air, and also includes an electrode pattern that allows droplets to pass over dried sample spots. MS results from these devices are of good quality.

Nichols *et al.* used the electro-wetting concept first to mix a droplet containing the substrate with a droplet containing the enzyme (*p*-nitrophenyl phosphate and YOP51 protein tyrosine phosphatase, respectively), quench it with a third droplet containing dichloroacetic acid and finally add the matrix, ferulic acid in an acetonitrile–water mixture, in a fourth droplet [74]. The shortest reaction time that could be studied with this system was about 5 ms, which could be achieved by "stirring" the droplet using high-frequency AC electro-wetting [73]. Figure 7.15 shows some of the kinetic data obtained with this approach.

At the end of this chapter, the approach of Brivio and coworkers of using microreactor chips in the vacuum chamber of a MALDI-MS machine is worth mentioning [78, 79]. This approach allows real on-line monitoring of reaction kinetics by MALDI-MS, but with only one time point at a time. The procedure for measuring a complete reaction curve is too time consuming and complex to be of practical use, but with dedicated and reconfigured MS equipment may be an option for on-line studies.

The basic concept consists in placing a microfluidic chip with two inlets, which have been filled with the two reagents that will be used in the reaction, in the vacuum chamber of the MALDI-MS equipment. The two inlets are hermetically closed before introducing the chip in the vacuum. Due to the vacuum present at the outlet of the microchannel network on the chip, the two reactants are pulled through the microchannels, merge in a T-junction, mix and then pass through a microchannel that acts as a reaction coil, before the mixture leaves the chip. Since one of the two original reactant solutions contains a matrix compound, the mixture will crystallize at the outlet of the chip, due to fast evaporation of the solvent, by which also the reaction is quenched. The laser is focused at the chip outlet to analyze the products. The first generation allowed reaction times of about 0.2 s [78]; with a later generation, with a

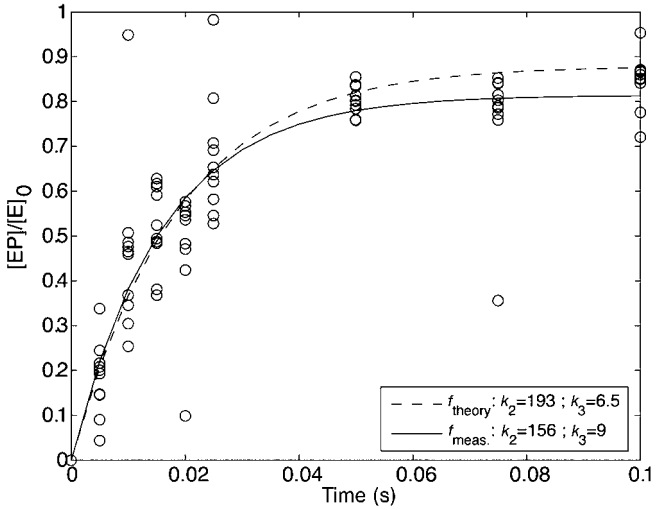

Figure 7.15 Ratio of the concentration of enzyme–product complex to that of the free enzyme as a function of reaction time. For details, see [74].

more complex channel network, a higher fluidic resistance and several monitoring windows that allowed more time points, the residence time was about 24 s, a factor of 100 longer [79].

7.4 Conclusions and Outlook

NMR microcoils, both solenoids and planar coils, have had impact on the capabilities of NMR as a detection scheme for in-flow chemistry. There is still growing interest in micro-NMR, due to the fact that scientists increasingly are challenged to do more with less sample. Recent studies focusing on liquid-flow profile imaging [80] and gas-flow profiling using remote detection NMR [81] give rise to the idea that probably micro-NMR is valuable not only for chemical spectroscopy. Advanced microimaging techniques can offer perspectives for studies of mixing and the space dependence of chemical reactions. Furthermore, chips with integrated microcoils and microfluidic channels on one substrate offer opportunities for sensitivity enhancement by use of on-board (CMOS) preamplifiers [82].

With respect to MS in combination with microreactors, it can be said that ESI is still the preferred method to couple microreactors (or microfluidics in general) to MS; however, recent developments show that the combination with MALDI is also feasible. A new development in the field of MALDI-MS is imaging, which up to now has mainly been used to study biological samples, such as tissue and in particular the effect of drugs on the metabolism in that tissue (see e.g. [83]). The

resolution of this technique is now ~100 µm, which is limited by the laser spot and therefore not yet suitable for use for in, for example, reaction kinetic studies on active catalytic sites, but new possibilities with this technique are evolving rapidly.

References

1 M.H. Levitt, *Spin Dynamics: Basics of Nuclear Magnetic Resonance*, John Wiley & Sons, Ltd, Chichester, **2001**.

2 J.H. Gross, *Mass Spectrometry. A Textbook*, Springer, Heidelberg, **2004**.

3 A. Abragam, *The Principles of Nuclear Magnetism*, Clarendon Press, Oxford, **1961**.

4 D.I. Hoult, R.E. Richards, *J. Magn. Reson.* **1976**, *24*, 71–85.

5 D.L. Olson, M.E. Lacey, J.V. Sweedler, *Anal. Chem.* **1998**, *70*, 257A–264A.

6 D.L. Olson, T.L. Peck, A.G. Webb, R. Magin, J.V. Sweedler, *Science* **1995**, *270*, 1967–1970.

7 N.N. Rao, *Electromagnetics*, Prentice Hall, Englewood Cliffs, NJ, **1992**.

8 F.D. Doty, Y. Entzminger, A. Yang, *Concepts Magn. Reson.* **1998**, *10*, 133–156.

9 B. Behnia, A.G. Webb, *Anal. Chem.* **1998**, *70*, 5326–5331.

10 N. Wu, T.L. Peck, A.G. Webb, R.L. Magin, J.V. Sweedler, *J. Am. Chem. Soc.* **1994**, *116*, 7929–7930.

11 N. Wu, T.L. Peck, A.G. Webb, R.L. Magin, J.V. Sweedler, *Anal. Chem.* **1994**, *66*, 3849–3857.

12 Protasis Magnetic Resonance Microsensors, Savoy, IL, USA, www.protasis.com.

13 D.L. Olson, J.A. Norcross, M. O'Neil-Johnson, P.F. Molitor, D.J. Detlefsen, A.G. Wilson, T.L. Peck, *Anal. Chem.* **2004**, *76*, 2966–2974.

14 W. Peti, J. Norcross, G. Eldridge, M. O'Neil-Johnson, *J. Am. Chem. Soc.* **2004**, *126*, 5873–5878.

15 A.A. Jansma, T. Chuan, R.W. Albrecht, D.L. Olson, T.L. Peck, B.H. Geierstanger, *Anal. Chem.* **2005**, *77*, 6509–6515.

16 R.J. Lewis, M.A. Bernstein, S.J. Duncan, C.J. Sleigh, *Magn. Reson. Chem.* **2005**, *43*, 783–789.

17 N.J.C. Bailey, I.R. Marshall, *Anal. Chem.* **2005**, *77*, 3947–3953.

18 T.L. Peck, R.L. Magin, J. Kruse, M. Feng, *IEEE Trans. Biomed. Eng.* **1994**, *41*, 706–709.

19 J.D. Trumbull, I.K. Glasgow, D.J. Beebe, R.L. Magin, *IEEE Trans. Biomed. Eng.* **2000**, *47*, 3–7.

20 S. Eroglu, S.C. Grant, G. Friedman, R.L. Magin, *First Annual International IEEE–EMBS Special Topic Conference on Microtechnologies in Medicine and Biology*, 12–14 October **2000**, Lyon.

21 S. Eroglu, B. Gimi, B. Roman, G. Friedman, R.L. Magin, *IEEE Trans. Magn.* **2001**, *37*, 2787–2789.

22 J. Dechow, A. Forchel, T. Lanz, A. Haase, *Microelectron. Eng.* **2000**, *53*, 517–519.

23 C. Massin, G. Boero, F. Vincent, J. Abenhaim, P.A. Besse, R.S. Popovic, *Sens. Actuators A* **2002**, *97–98*, 280–288.

24 C. Massin, F. Vincent, A. Homsy, K. Ehrmann, G. Boero, P.A. Besse, A. Daridon, E. Verpoorte, N.F. de Rooij, R.S. Popovic, *J. Magn. Reson.* **2003**, *164*, 242–255.

25 A.G. Webb, *J. Pharm. Biomed. Anal.* **2005**, *38*, 892–903.

26 J.H. Walton, J.S. de Ropp, M.V. Shutov, A.G. Goloshevsky, M.J. McCarthy, R.L. Smith, S.D. Collins, *Anal. Chem.* **2003**, *75*, 5030–5036.

27 R.R.A. Syms, M.M. Ahmad, I.R. Young, Y. Li, J. Hand, D. Gilderdale, *J. Micromech. Microeng.* **2005**, *15*, 1–9.

28 K. Ehrmann, N. Saillen, F. Vincent, M. Stettler, M. Jordan, F.M. Wurm, P.A. Besse, R. Popovic, *Lab Chip* **2007**, *7*, 373–380.

29 D.A. Laudr Jr, C.L. Wilkins, *Anal. Chem.* **1984**, *56*, 2471–2475.

30 H.C. Dorn, *Anal. Chem.* **1984**, *56*, 747A–758A.

31 K. Albert (ed.), *On-line LC–NMR and Related Techniques*, John Wiley & Sons, Ltd, Chichester, **2002**.

32 N. Wu, A. Webb, T.L. Peck, J.V. Sweedler, *Anal. Chem.* **1995**, *67*, 3101–3107.

33 S.A. Korhammer, A. Bernreuther, *Fresenius' J. Anal. Chem* **1996**, *354*, 131–135.

34 P. Gfrörer, J. Schewitz, K. Pusecker, L.H. Tseng, K. Albert, E. Bayer, *Electrophoresis* **1999**, *20*, 3–8.

35 D.L. Olson, M.E. Lacey, A.G. Webb, J.V. Sweedler, *Anal. Chem.* **1999**, *71*, 3070–3076.

36 J.F. McGarrity, C.A. Ogle, Z. Brich, H.-R. Loosli, *J. Am. Chem. Soc.* **1985**, *107*, 1810–1815.

37 C.A. Fyfe, S.W.H. Damji, A. Koll, *J. Am. Chem. Soc.* **1979**, *101*, 951–955.

38 L. Ciobanu, D.A. Jayawickrama, X. Zhang, A.G. Webb, J.V. Sweedler, *Angew. Chem. Int. Ed. Engl.* **2003**, *42*, 4669–4672.

39 H. Wensink, F. Benito-Lopez, D.C. Hermes, W. Verboom, J.G.E. Gardeniers, D.N. Reinhoudt, A. van den Berg, *Lab Chip* **2005**, *5*, 280–284.

40 M. Nakakoshi, M. Ueda, S. Sakurai, K. Asakura, H. Utsumi, O. Miyata, T. Naito, Y. Takahashi, *Magn. Reson. Chem.* **2007**, *45*, 989–992.

41 Y. Takahashi, R. Sakai, M. Nakakoshi, S. Sakurai, R. Tanaka, H. Suematsu, H. Utsumi, T. Kitamori, in *The 10th International Conference on Miniaturized Systems for Chemical and Life Sciences (uTas 2006)*, 5–9 November **2006**, Tokyo, pp. 879–881.

42 N.A.J. van Nuland, V. Forge, J. Balbach, C.M. Dobson, *Acc. Chem. Res.* **1998**, *31*, 773–780.

43 H. Roder, G.A. Elove, S. Ramachandra, *Mechanisms of Protein Folding*, 2nd ed., Oxford University Press, New York, **2000**.

44 M. Kakuta, D.A. Jayawickrama, A.M. Wolters, A. Manz, J.V. Sweedler, *Anal. Chem.* **2003**, *75*, 956–960.

45 F.G. Bessoth, A.J. deMello, A. Manz, *Anal. Commun.* **1999**, *36*, 213–215.

46 G.J. Dear, J. Ayrton, R. Plumb, B.C. Sweatman, I.M. Ismail, I.J. Fraser, P.J. Mutch, *Rapid Commun. Mass Spectrom.* **1998**, *12*, 2023–2030.

47 F.S. Pullen, A.G. Swanson, M.J. Newman, D.S. Richards, *Rapid Commun. Mass Spectrom.* **1995**, *9*, 1003–1006.

48 R.R. Ernst, G. Bodenhausen, A. Wokaun, *Principles of Nuclear Magnetic Resonance in One and Two Dimensions*, Clarendon Press, Oxford, **1987**.

49 K. Wüthrich, *Methods Enzymol.* **1989**, *177*, 125–131.

50 X. Ouyang, L. Bednarova, R.S. Besser, P. Ho, *AIChE J.* **2005**, *51*, 1758–1772.

51 U.J. Quaade, S. Jensen, O. Hansen, *Rev. Sci. Instrum.* **2004**, *75*, 3345–3347.

52 P. Claus, D. Hönicke, T. Zechet, *Catal. Today* **2001**, *67*, 319–339.

53 S. Senkan, S. Ozturk, *Angew. Chem. Int. Ed.* **1999**, *38*, 2794–2799.

54 J.A. Olivares, N.T. Nguyen, C.R. Yonker, R.D. Smith, *Anal. Chem.* **1987**, *59*, 1230–1232.

55 J.F. Banks Jr, C.M. Whitehouse, *Methods Enzymol.* **1996**, *270*, 486–519.

56 R.C. Beavis, B.T. Chait, *Methods Enzymol.* **1996**, *270*, 519–551.

57 M. Karas, F. Hillenkamp, *Anal. Chem.* **1988**, *60*, 2299–2301.

58 A. Liesener, U. Karst, *Anal. Bioanal. Chem.* **2005**, *382*, 1451–1464.

59 R.D. Oleschuk, J.D. Harrison, *Trends Anal. Chem.* **2000**, *19*, 379–388.

60 R.S. Ramsey, J.M. Ramsey, *Anal. Chem.* **1997**, *69*, 1174–1178.

61 Q. Xue, F. Foret, Y.M. Dunayevskiy, P.M. Zavracky, N.E. McGruer, B.L. Karger, *Anal. Chem.* **1997**, *69*, 426–430.

62 D. Figeys, Y. Ning, R. Aebersold, *Anal. Chem.* **1997**, *69*, 3153–3160.

63 A. Desai, Y.-C. Tai, M.T. Davis, T.D. Lee, in *Technical Digest of the 1997 International Conference on Solid- State Sensors and Actuators (Transducers '97), Chicago*, 16–19 June **1997**, pp. 927–930.

64 G.A. Schultz, N.C. Corso, S.J. Prosser, S. Zhang, *Anal. Chem.* **2000**, *72*, 4058–4063.

65 H. Yin, K. Killeen, R. Brennen, D. Sobek, M. Werlich, T. van de Goor, *Anal. Chem.* **2005**, *77*, 527–533.

66 Q. Xue, F. Foret, Y.M. Dunayevskiy, P.M. Zavracky, N.E. McGruer, B.L. Karger, *Anal. Chem.* **1997**, *69*, 426–430.

67 H. Liu, C. Felten, Q. Xue, B. Zhang, P. Jedrzejewski, B.L. Karger, F. Foret, *Anal. Chem.* **2000**, *72*, 3303–3310.

68 F. Foret, P. Kusý, *Electrophoresis* **2006**, *27*, 4877–4887.

69 M. Brivio, R.E. Oosterbroek, W. Verboom, A. van den Berg, D.N. Reinhoudt, *Lab Chip* **2005**, *5*, 1111–1122.

70 M. Brivio, A. Liesener, R.E. Oosterbroek, W. Verboom, U. Karst, A. van den Berg, D.N. Reinhoudt, *Anal. Chem.* **2005**, *77*, 6852–6856.

71 M. Brivio, R.E. Oosterbroek, W. Verboom, M.H. Goedbloed, A. van den Berg, D.N. Reinhoudt, *Chem. Commun.* **2003**, 1924–1925.

72 V. Spikmans, S.J. Lane, B. Leavens, A. Manz, N.W. Smith, *Rapid Commun. Mass Spectrom.* **2002**, *16*, 1377–1388.

73 K.P. Nichols, J.G.E. Gardeniers, in *Proceedings of the 10th International Conference on Miniaturized Systems for Chemistry and Life Sciences (MicroTAS 2006)*, Tokyo, 5–9 November **2006**, pp. 582–584.

74 Nichols, J.G.E. Gardeniers, in *Proceedings of the 10th International Conference on Miniaturized Systems for Chemistry and Life Sciences (MicroTAS 2006)*, Tokyo, 5–9 November **2006**, pp. 786–788.

75 Moon, A.R. Wheeler, R.L. Garrell, J.A. Loo, C.J. Kim, *Lab Chip* **2006**, *6*, 1213–1219.

76 A.R. Wheeler, H. Moon, C.-J. Kim, J.A. Loo, R.L. Garrell, *Anal. Chem.* **2004**, *76*, 4833–4838.

77 A.R. Wheeler, H. Moon, C.A. Bird, R.R.O. Loo, C.-J. Kim, J.A. Loo, R.L. Garrell, *Anal. Chem.* **2005**, *77*, 534–540.

78 M. Brivio, R.H. Fokkens, W. Verboom, D.N. Reinhoudt, N.R. Tas, M.H. Goedbloed, A. van den Berg, *Anal. Chem.* **2002**, *74*, 3972–3976.

79 M. Brivio, N. Tas, M.H. Goedbloed, H.J.G.E. Gardeniers, W. Verboom, A. van den Berg, D.N. Reinhoudt, *Lab Chip* **2005**, *5*, 378–381.

80 A.G. Goloshevsky, J.H. Walton, M.V. Shutov, J.S. de Ropp, S.D. Collins, M.J. McCarthy, *Meas. Sci. Technol.* **2005**, *16*, 505–512.

81 C. Hilty, E.E. McDonnel, J. Granwehr, K.L. Pierce, S.-I. Han, A. Pines, *Proc. Natl. Acad. Sci. USA* **2005**, *102*, 14960–14963.

82 T. Cherifi, N. Abouchi, G.-N. Lu, L. Bouchet-Fakri, L. Quiquerez, B. Sorli, J.-F. Chateaux, M. Pitaval, P. Morin, *IEEE Trans. Circ. Syst-I: Reg. Pap.* **2005**, *52*, 2576–2583.

83 S.L. Luxembourg, T.H. Mize, L.A. McDonnell, R.M.A. Heeren, *Anal. Chem.* **2004**, *76*, 5339–5344.